



Supercapacitor Separators and Polypyrrole Composites

Colin G. Cameron

Shayla M. Fitzsimmons

Defence R&D Canada – Atlantic

Technical Memorandum
DRDC Atlantic TM 2008-219
December 2008

This page intentionally left blank.

Supercapacitor Separators and Polypyrrole Composites

Colin G. Cameron
Shayla M. Fitzsimmons

Defence R&D Canada – Atlantic

Technical Memorandum

DRDC Atlantic TM 2008-219

December 2008

Principal Author

Original signed by Colin Cameron

Colin G. Cameron

Approved by

Original signed by Leon Cheng

Leon Cheng
Section Head / DL(A)

Approved for release by

Original signed by Ron Kuwahara for

Calvin Hyatt
Chair/ Document Review Panel

© Her Majesty the Queen in Right of Canada as represented by the Minister of National Defence, 2008

© Sa Majesté la Reine (en droit du Canada), telle que représentée par le ministre de la Défense nationale, 2008

Abstract

The current trend of military forces worldwide is an increasing dependence on electrical power, and the Canadian Forces is no exception. Current technology, such as chemical sensors, radios, and portable computers, as well as rapidly emerging weaponry such as electromagnetic guns and directed energy weapons, demand increasingly sophisticated provision of electrical energy. Supercapacitors, for example, are ideally suited to supply large pulses of energy, and it is within the DRDC Technology Investment Fund project on supercapacitor materials that the current research has been undertaken.

This document reports the work of a summer student who studied two fundamental aspects of novel energy provision. First, a comparison of the low temperature performance of two different types of supercapacitor separator represents this lab's initial investigation into this niche area. It was found that a fixed pore separator outperforms a proton exchange membrane at low temperatures. Second, work with nanostructured polypyrrole composites builds on our earlier work in this interesting material, one which has numerous potential applications, including energy storage. Several concept structures are reported, including an all-polymer wire.

Résumé

Les armées du monde, y compris les forces canadiennes, jouissent d'une dépendance augmentante sur l'énergie électrique. Les technologies modernes tels que les capteurs chimiques, les radios, les ordinateurs portables, ainsi que les armements du futur, dont les fusils électromagnétiques et les armements d'énergie directe, exigent une provision d'énergie électrique de plus en plus complexe. Les supercondensateurs, par exemple, peuvent fournir des énormes impulsions d'énergie, et c'est dans le cadre du programme Fonds d'investissement en technologie (FIT) à RDDC sur les supercondensateurs que les présents recherches ont eu lieu.

Ce rapport résume les recherches d'une étudiante qui a examiné la provision d'énergie électrique sous deux de ses aspects. Premièrement, on a comparé le fonctionnement de deux types de couches de séparation de supercondensateur à température basse. On a trouvé qu'une couche à pore fixe fonctionne mieux qu'une couche de membrane à échange de protons. Deuxièmement, des expériences sur des matériaux composites de polypyrrole à nanostructure continuent nos recherches sur ce matériau intéressant qui a de nombreuses applications, y compris le stockage d'énergie. Quelques structures de concept sont élaborées, dont un fil électrique construit de polymère.

This page intentionally left blank.

Executive summary

Supercapacitor Separators and Polypyrrole Composites

Colin G. Cameron, Shayla M. Fitzsimmons; DRDC Atlantic TM 2008-219; Defence R&D Canada – Atlantic; December 2008.

Background: This document presents the work of a summer student in the Dockyard Laboratory (Atlantic). It covers research in two separate areas of interest: supercapacitor materials and polypyrrole composites. The supercapacitor portion of the report consists of a preliminary investigation on the effects of separator material on the low temperature performance of the device. The polypyrrole section describes experiments intended to improve our understanding of the conditions that influence the underlying polymerization reaction.

Principal Results: It was found (i) that a fixed pore cellulose-type separator membrane quickly outperformed a proton exchange membrane when the temperature of the cell fell below around 0°C, and (ii) that moisture in the reaction solution has serious deleterious effects on the conductivity of the resulting polymer. Additionally, flexible polypyrrole composites in the form of “plastic wires” were demonstrated.

Significance of Results: The low temperature performance of supercapacitors is an area of vital strategic significance if Canada’s interest in Arctic sovereignty remains a priority. Studies such as this lay the foundation for creating electrical power sources suited to such an environment.

Conducting polymer composites are materials of fundamental interest for a number of foreseeable applications. These include supercapacitor materials, adaptive camouflage, and sensors. Through understanding the factors that influence the cascade polymerization, new compounds and structures can be created. This is illustrated in the present work by conductive hollow microtubes and by a plastic wire.

Future Work: The low temperature performance is one aspect of the supercapacitor TIF program, and research continues in this area. It is hoped that a low temperature proof-of-concept cell will be demonstrated soon. Likewise, the fundamental aspects of the cascade polymerization technique continue to be elucidated.

Sommaire

Supercapacitor Separators and Polypyrrole Composites

Colin G. Cameron, Shayla M. Fitzsimmons ; DRDC Atlantic TM 2008-219 ; R & D pour la défense Canada – Atlantique ; décembre 2008.

Contexte : Ici on présente les résultats obtenus par une étudiante au laboratoire du chantier navale (Atlantique). Deux sujets sont examinés : les matériaux pour supercondensateurs et des composites de polypyrrole. Le premier section s'occupe du fonctionnement des couches de séparation aux températures basses. Le deuxième décrit des expériences qui visent à améliorer notre compréhension des conditions qui influencent la réaction chimique du polymérisation.

Résultats principaux : On a trouvé (i) qu'une membrane en cellulose aux pores invariants fonctionne mieux qu'une membrane à échange de protons quand la température baisse au moins d'environ 0°C, et (ii) que du l'eau dans la solution réactive peut gravement affecter la conductivité du polymère. Par ailleurs, on a démontré des composites flexibles de polypyrrole comme fils électriques en plastique.

Portée des Résultats : Le fonctionnement des supercondensateurs aux températures basses est un sujet stratégique important si la souveraineté arctique continue d'être une priorité. Les études tel que ci posent les fondations de la création des nouvelles technologies d'énergie visés à un environnement froid.

Les composites de polymère conducteur sont des matériaux fondamentalement intéressants pour de nombreuses applications, tel que le stockage d'énergie (électrodes de supercondensateurs, par exemple), le camouflage adaptif, et les capteurs. Par comprendre les facteurs qui contrôlent le polymérisation, on pourra créer de nouveaux matériaux. On a démontré quelques exemple ici : des microtuyaux conducteurs et un fil électrique en plastique.

Recherches futures : Le fonctionnement des condensateurs aux températures basses est un aspect important du programme FIT, et on continuera à l'étudier. On tente à démontrer bientôt un élément de supercondensateur optimisé pour fonctionner dans le froid. De plus, on continuera à élucider la réaction de polymérisation cascade.

Table of contents

Abstract	i
Résumé	i
Executive summary	iii
Sommaire	iv
Table of contents	v
List of figures	vii
List of tables	viii
1 Low Temperature Assessment of Supercapacitor Separator Materials	1
1.1 Background	1
1.2 Experimental	2
1.2.1 Cell design	2
1.2.2 Impedance methods	2
1.2.3 Galvanostatic discharge	5
1.3 Results	6
2 Polypyrrole Composites and Coatings	8
2.1 Background	8
2.2 Common Experimental	9
2.2.1 Equipment	9
2.2.2 Materials	9
2.3 Coated Poly(vinyl alcohol) Threads	10
2.3.1 Background	10
2.3.2 Coating methods	10
2.3.2.1 preparation method one	10

2.3.2.2	preparation method two	10
2.3.2.3	preparation method three	10
2.3.3	Results	11
2.3.3.1	method one	11
2.3.3.2	methods two and three	11
2.4	Glass Slides	14
2.4.1	Background	14
2.4.2	Methods	14
2.4.3	Results	15
2.4.4	Conclusions	17
2.5	Polyurethane Composites	17
2.5.1	Background	17
2.5.2	Method	17
2.5.3	Results	17
2.5.4	Example applications of polypyrrole composites	18
2.6	Porous Polypyrrole	18
2.6.1	Background	18
2.6.2	Method	19
2.6.2.1	experimental	19
2.6.2.2	electrochemistry	19
2.6.3	Cyclic voltammetry	19
2.6.4	Impedance spectroscopy	21
2.7	Polypyrrole Summary	22
	Symbols and Abbreviations	23

References	25
Distribution list	27

List of figures

Figure 1: Ragone plot of a fuel cell, battery, conventional capacitor and supercapacitor.	1
Figure 2: Schematic model of the supercapacitor test cell.	2
Figure 3: (a) Ideal Nyquist plot of a surface-bound conducting polymer, and (b) the dual transmission line equivalent circuit model.	3
Figure 4: Nyquist plot analysis of a carbon cloth supercapacitor having a paper separator, recorded at 20°C.	4
Figure 5: Capacitance data for a carbon cloth supercapacitor having a paper separator, recorded at 20°C : (a) Imaginary impedance vs. reciprocal frequency, and (b) capacitance vs. resistance.	4
Figure 6: Temperature dependence of the galvanostatic discharge (100 mA) of a carbon cloth capacitor with a paper separator.	5
Figure 7: Temperature-dependent response: (a) and (b) imaginary impedance vs. reciprocal frequency and specific capacitance vs. resistance, respectively, for a cell with a paper separator; (c) and (d) imaginary impedance vs. reciprocal frequency and specific capacitance vs. resistance, respectively, for a cell with a Nafion separator.	6
Figure 8: Ragone plots at varying temperature for capacitors containing (a) a paper separator, and (b) a Nafion separator.	8
Figure 9: Constant current discharge profiles for a paper-separated capacitor at 20°C.	9
Figure 10: SEM images of PVA threads coated with five layers of polypyrrole, using the method as described in Section 2.3.2.1: (a) 1300×, thread not rinsed with MeOH between layers, PVA thread not dissolved; (b) 1140×, thread rinsed with MeOH between layers, PVA thread not dissolved; (c) 1100×, thread not rinsed with MeOH between layers, PVA thread dissolved; (d) 1200×, thread rinsed with MeOH between layers, PVA thread dissolved.	12

Figure 11:	PVA threads coated in 30 layers of polypyrrole, and neither rinsed with methanol between layers: (a) 1000×, PVA thread dissolved; (b) 1000×, PVA thread not dissolved.	13
Figure 12:	Examples of non-metallic wiring. Left: An FeCl ₃ -doped polypyrrole film coated on a glass slide. Right: a length of freestanding polypyrrole composite “wire”.	18
Figure 13:	(a) Ideal voltammetric response of an RC circuit. When $R = 0$, the trace becomes rectangular, in accordance with Equation 9. (b) Representative cyclic voltammogram of polypyrrole on a glassy carbon disc electrode in MeCN/LiClO ₄ , $v = 10$ mV/s.	20
Figure 14:	Representative degradation of a PPy film upon cycling at elevated potentials.	21
Figure 15:	Variation in R_i with potential.	22

List of tables

Table 1:	Summary of capacitance and resistance values for capacitors having paper or Nafion separators, over a range of temperatures.	7
Table 2:	Resistance (over 1 cm) of various polypyrrole-coated poly vinyl alcohol threads as measured with a multimeter. Each thread was coated with 30 layers of polypyrrole. None of the threads was rinsed with MeOH between coats.	13
Table 3:	Multimeter (MM) and four-point probe resistance of treated polypyrrole films on glass slides, before and after rinsing with methanol.	16
Table 4:	Capacitance and ionic resistance of polypyrrole films of varying composition.	20

1 Low Temperature Assessment of Supercapacitor Separator Materials

1.1 Background

The DRDC report *Technology Trends, Threats, Requirements, and Opportunities Study on Advanced Power Sources for the Canadian Forces in 2020* [1] identifies key issues for the delivery of electrical power to CF operations over the near- to medium-term. Supercapacitors were noted for their ability to provide pulses of power and load-leveling of lower power sources. The Ragone plot presented in Figure 1 illustrates typical specific power and specific energy for several sources of electrical energy, and it presents a technology gap. Batteries and fuel cells store a lot of energy, but are unable to discharge the energy very quickly. On the other hand, conventional capacitors contain very little energy, but are able to discharge very quickly, providing brief transients of high power. Supercapacitors provide performance that bridges batteries and capacitors, providing moderate amounts of energy at reasonably high rates, and for this reason they are attractive for designing more rational and efficient electrical power distribution for certain applications and the pulses of high power necessary for others.

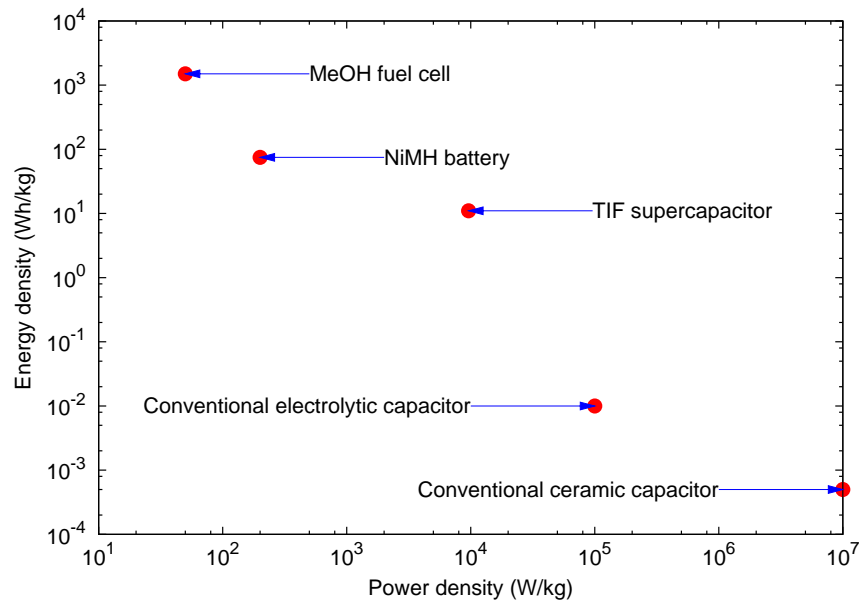


Figure 1: Ragone plot of a fuel cell, battery, conventional capacitor and supercapacitor.

The DRDC Technology Investment Fund (TIF) program on supercapacitor materials (WBE 12sz07) has been aiming to produce better devices through the design of better constituent materials. One aspect of the program is to examine ways of achieving useful performance in a cold environment.

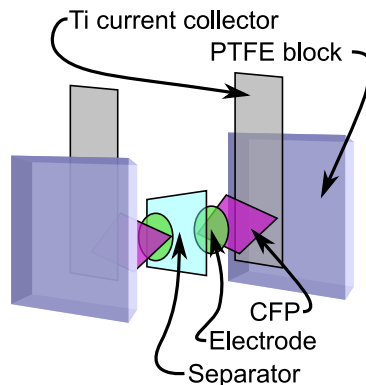


Figure 2: Schematic model of the supercapacitor test cell.

This section presents a preliminary examination of the low temperature performance of supercapacitor prototypes having a separator consisting of two fundamentally different materials: A non-porous proton exchange membrane and a fixed-pore cellulose-based separator taken from a Maxwell commercial supercapacitor.

1.2 Experimental

1.2.1 Cell design

Discs of Spectracarb activated carbon fabric (type 2225) were used as the capacitor electrodes without modification. These were held in a sandwich-like configuration between a pair of PTFE blocks, as illustrated in Figure 2. A small strip of Spectracarb 2050L carbon fibre paper was positioned between each electrode and its corresponding titanium current collector to improve electrical contact. The contact surface of the collectors were sanded with emery cloth before assembly to remove excess oxide. Finally, the assembly was fastened with steel bolts.

1.2.2 Impedance methods

Impedance spectroscopy is a useful tool in the study of charge migration in electrochemical systems, including supercapacitors and conducting polymer films. This method allows for the extraction of individual phenomena that comprise the overall electrochemical response [2–5]. For instance, it has been shown that the ideal complex plane response of a thin electroactive film (Figure 3a) has two distinct regions: a high frequency $\sim 45^\circ$ Warburg-type charge migration line and a nearly vertical low frequency capacitive region. The response can be modeled by a finite transmission line equivalent circuit, shown in an abridged form in Figure 3b.

In the case where electronic resistance R_e is relatively low, the model simplifies, and the ionic resistance R_i can be determined fairly easily from the x -axis intercepts of the low-

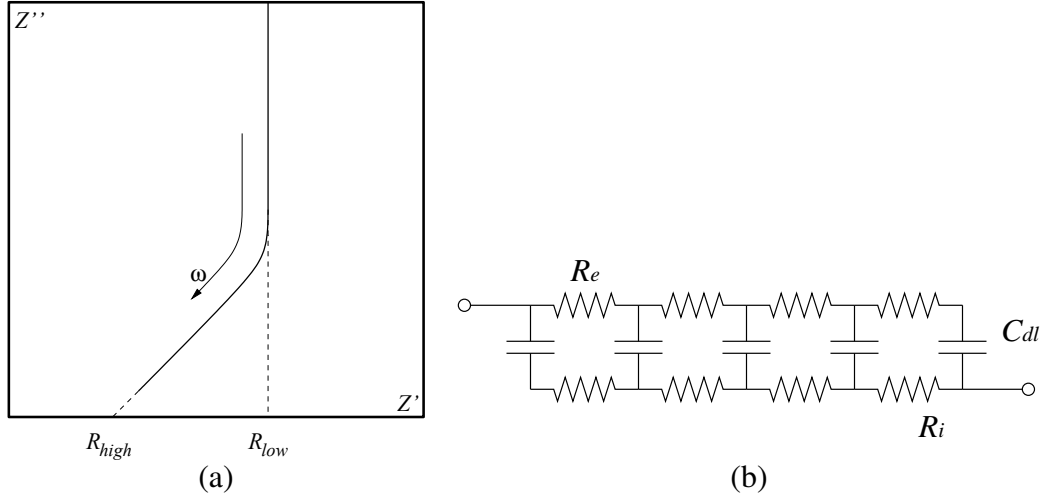


Figure 3: (a) Ideal Nyquist plot of a surface-bound conducting polymer, and (b) the dual transmission line equivalent circuit model.

and high-frequency data:

$$R_i = 3(R_{low} - R_{high}) \quad (1)$$

An example illustrated in Figure 4. The high frequency x -axis intercept, R_{high} , yields the Equivalent Series Resistance (ESR) of the cell, which includes the resistance of the membrane, the leads and clips, the electronic resistances of the titanium collectors and carbon materials, and the various contact resistances in the assembly. The absence of a small semicircle at the beginning of the high frequency data indicates that there was no significant charge transfer resistance between the electrode and the Ti current collector (through the CFP layer).

Capacitance C is related to the imaginary impedance Z'' through the following equation:

$$C = 1/\omega Z'' \quad (2)$$

where ω is in rad/s.

Low frequency capacitance can be extracted from the Z'' data from the relationship of Equation 2; a plot of $-Z''$ vs. $1/\omega$ (in rad/s) has slope $1/C$, illustrated in Figure 5a. Alternatively, the same information, albeit less precise, is yielded as the horizontal asymptote on a C vs. resistance (Z') plot, as shown in Figure 5b. The latter plot is useful for comparing interfacial resistances [6], which are related to the initial slope of the data.

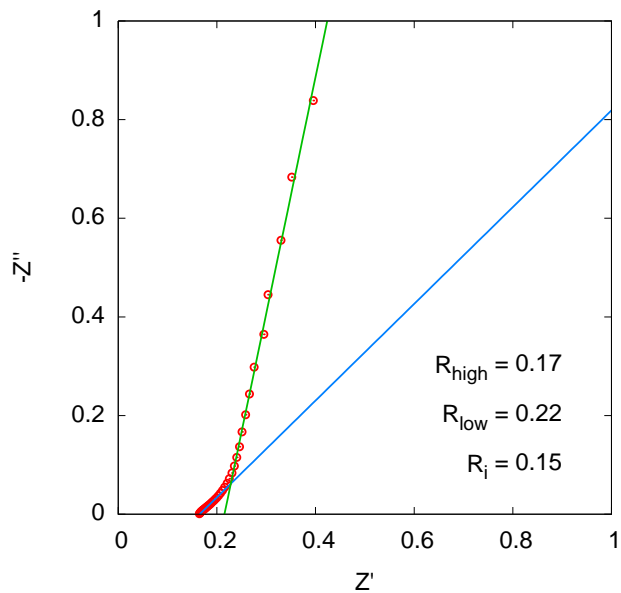


Figure 4: Nyquist plot analysis of a carbon cloth supercapacitor having a paper separator, recorded at 20°C.

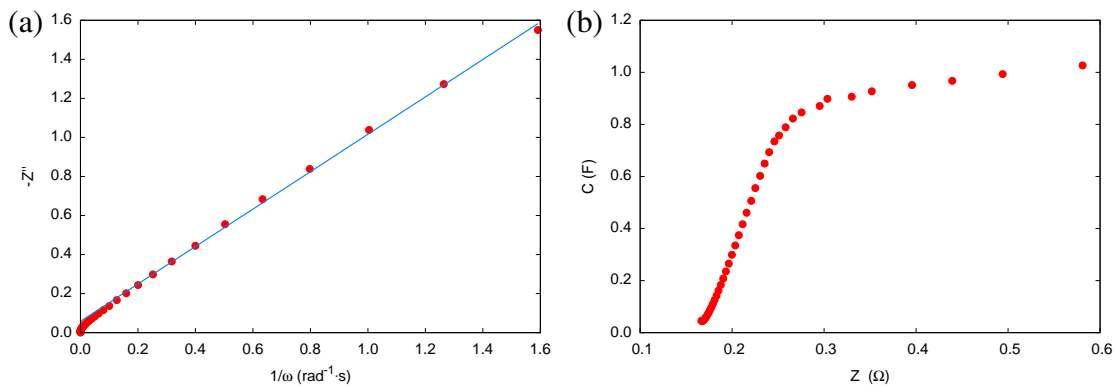


Figure 5: Capacitance data for a carbon cloth supercapacitor having a paper separator, recorded at 20°C : (a) Imaginary impedance vs. reciprocal frequency, and (b) capacitance vs. resistance.

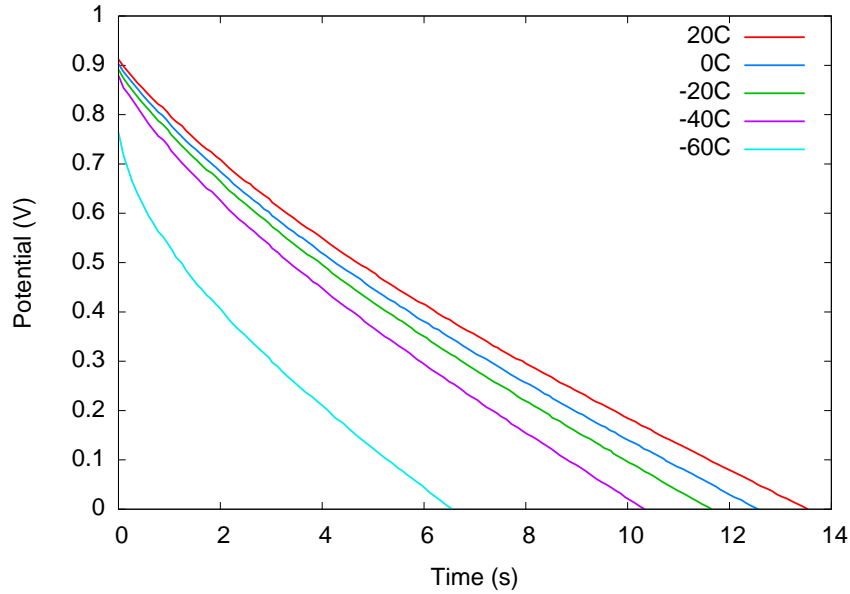


Figure 6: Temperature dependence of the galvanostatic discharge (100 mA) of a carbon cloth capacitor with a paper separator.

1.2.3 Galvanostatic discharge

The constant-current discharge of the capacitors is a convenient way to assess their performance under realistic conditions. The constant diagonal slope of the V vs. time plot is characteristic of an ideal capacitor when current ($i \equiv dQ/dt$) is constant, because

$$V = \frac{Q}{C} \quad (3)$$

$$\frac{dV}{dt} = \left(\frac{1}{C}\right) \frac{dQ}{dt} \quad (4)$$

Example discharges at varying temperature are shown in Figure 6.

The power produced at any time is the product of current and voltage, $P = iV$. The integration of power with respect to time over the discharge period reveals the total available energy of the capacitor under such conditions:

$$E = \int P dt \quad (5)$$

$$= i \int V dt \quad (6)$$

Equation 6 can be solved numerically for a constant-current discharge by integrating the voltage over the discharge time and multiplying by the constant current.

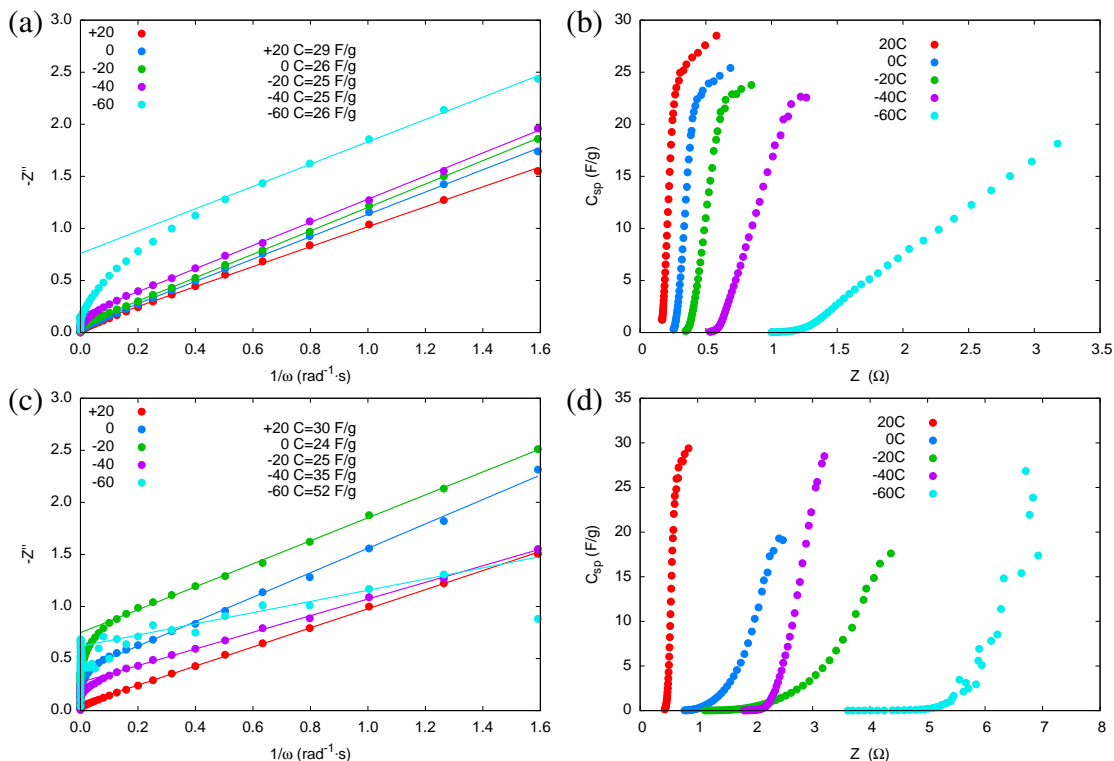


Figure 7: Temperature-dependent response: (a) and (b) imaginary impedance vs. reciprocal frequency and specific capacitance vs. resistance, respectively, for a cell with a paper separator; (c) and (d) imaginary impedance vs. reciprocal frequency and specific capacitance vs. resistance, respectively, for a cell with a Nafion separator.

Average power P_{avr} is obtained by dividing the total energy by the total discharge time, and the capacitance C equals the charge passed (the product of current and discharge time) divided by the voltage change from $t = 0$. By discharging a cell at different currents, a Ragone plot (power vs. energy) may be constructed.

1.3 Results

Table 1 summarizes resistance and capacitance data as extracted from impedance experiments. The specific capacitance does not appear to vary meaningfully with temperature or depend on the nature of the separator. The latter is not surprising, since there is no direct interaction between the separator and the electrochemical double layer that leads to capacitance. The double layer capacitance is, however, affected by temperature, since the dielectric constant ϵ of the solvent tends to drop at lower temperatures and the effective thickness of the layer also decreases. The effect is not a major one, being around 10–15% over 60°C at a mercury electrode [7], and not even detectable in the current data. The slopes in Figures 7(a) and (c) are reciprocal capacitance, and remain more-or-less parallel throughout the temperature range. The same should hold true for constant current dis-

Table 1: Summary of capacitance and resistance values for capacitors having paper or Nafion separators, over a range of temperatures.

Temperature (°C)	Paper			Nafion-117		
	ESR (Ω)	R_i (Ω)	C_{sp} (imp) (F/g)	ESR (Ω)	R_i (Ω)	C_{sp} (imp) (F/g)
20	0.17	0.15	29	0.35	0.29	30
0	0.25	0.30	26	0.45	1.73	24
-20	0.28	0.51	25	0.63	6.82	25
-40	0.37	0.91	25	1.30	3*	35
-60	0.66	> 6*	26	2.57	7.8*	52

* Estimated from graph

charges, such as the one presented in Figure 6, and similar results have been shown for commercial capacitors manufactured by Maxwell and Panasonic, as discussed in Chapter 20 of reference 7.

Generally, electrolyte conductivity falls off rapidly with decreasing temperature due to increased solvent viscosity and lower ion dissociation. This leads to increased ESR (including ionic resistance R_i) and hence diminished power. Increased resistances at lower temperatures are noted in Table 1. The increased resistance is far more pronounced in Nafion, the ion exchange membrane, than in the fixed-pore paper. Ionic resistance dominates in both cases, presumably reflecting the restriction to ion transport through the separator. Clearly the paper-based separator out-performs the solid-state Nafion membrane at lower temperatures, to the point where the Nafion data at -40°C and below should be considered unreliable. Other contributions to overall resistance also increase at lower temperature, again Nafion exhibiting the greater losses. The slopes in Figures 7(b) and (d) suggest that interfacial resistances increase more rapidly for Nafion, although the reasons for this are not currently clear.

The effects of increased resistance are evident in the Ragone plots in Figure 8. Available energy rolls off at higher power loads, as expected. The effect is so dramatic for Nafion that the cell was unable to deliver higher powers at lower temperature, hence the missing data at the lower right of Figure 8(b). The data in both plots has a problem, however, arising from a procedural error: incomplete charging led to an artificially diminished total available energy. The effects of this are most evident in the low-power tests, towards the left of each graph, producing an unusual drop. Examination of the discharge curves (*e.g.*, Figure 9, plotted with a log(time) axis for clarity) reveals an abnormally low initial voltage. It is customary to see an iR drop associated with the ESR of the cell, but the loss of nearly 0.06 V for the 1 mA discharge and the identical loss at 100 mA indicate that cell had not been charged fully to 1.0 V. Nonetheless, the comparisons between Figures 8(a) and (b) are valid, since identical charging sequences were used in all cases.

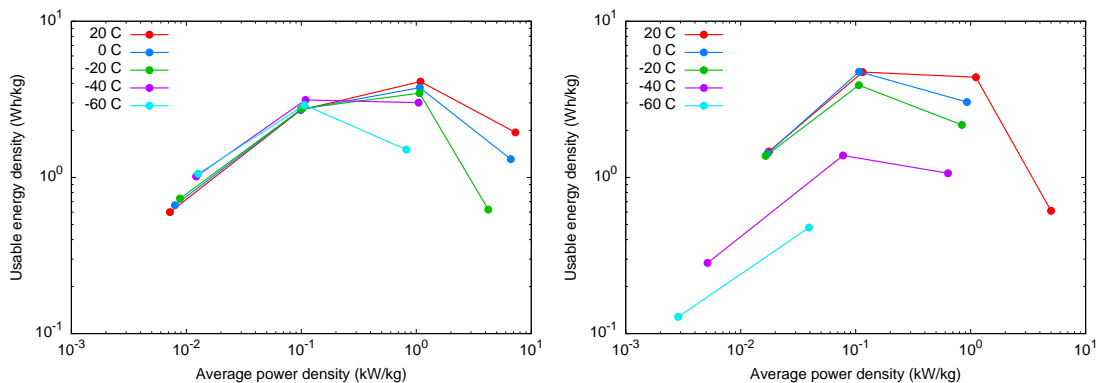


Figure 8: Ragone plots at varying temperature for capacitors containing (a) a paper separator, and (b) a Nafion separator.

To summarize, Nafion is a very poor performer at lower temperature, presumably due to restricted proton flux through the polymer. A fixed pore separator, such as the commercial supercapacitor paper used in the Maxwell devices, offers a more consistent response over a wide temperature range. This will be investigated further in the near future.

2 Polypyrrole Composites and Coatings

2.1 Background

Freund's polymerization method [8,9] is a novel way of generating conducting polymers in a processible way, producing materials that are of interest to DRDC [10–16]. The proposed mechanism involves the use of a dilute solution of monomer and a weak oxidant such that the active oxidized form of the monomer is in such low abundance that the polymerization reaction is kinetically inhibited. Evaporation of the solvent allows the buildup of the reactive form until a point where polymerization can begin, and the product forms. It is this inherent control over the polymerization process that presents the possibility of coating arbitrary surfaces or forming composites in ways that are impossible using the more conventional polymerization methods. The present work aims (i) to coat soluble templates with polypyrrole (PPy), (ii) to create interpenetrating polymer networks of polypyrrole and polyurethane, using the latter as an inert support for both the formation of porous structures (after removal of the polyurethane) and the creation of free-standing, all-polymer conductors, and (iii) to optimize the experimental conditions for polymerization.

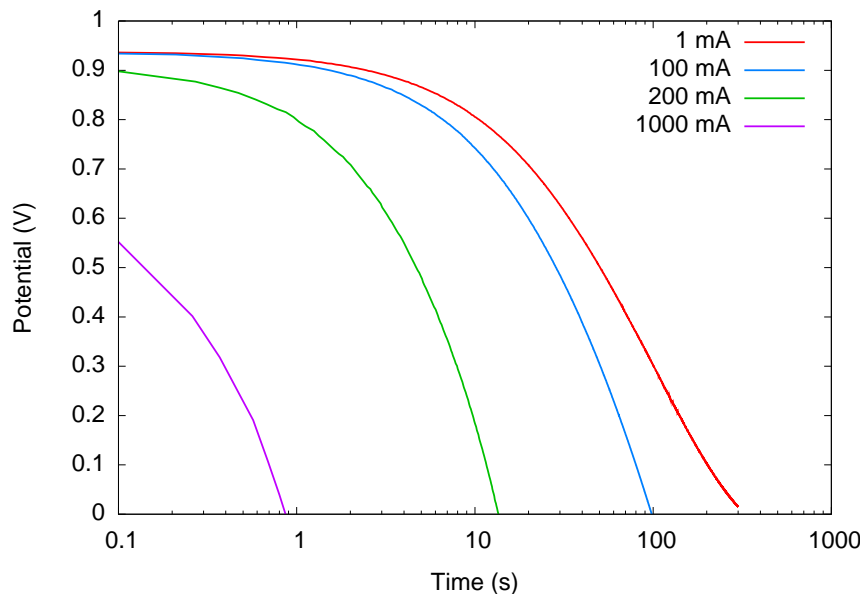


Figure 9: Constant current discharge profiles for a paper-separated capacitor at 20°C.

2.2 Common Experimental

2.2.1 Equipment

A Fluke 189 True RMS Multimeter and a Jandel Model RM3 Four-Point Probe were used to take resistance measurements of the polypyrrole films.

A Solartron SI1287 Electrochemical Interface and a Solartron SI1260 Impedance/Gain-Phase Analyzer were used to obtain the cyclic voltammogram and impedance data. Electrochemical studies were performed in a three-electrode configuration, using a saturated calomel (SCE) reference electrode.

Scanning electron microscopy (SEM) images were acquired on a LEO 1455VP microscope.

2.2.2 Materials

Phosphomolybdic acid hydrate (Fisher) was used as received; its molar mass was previously determined to be 2366 g/mol [14]. Pyrrole was obtained from either Aldrich or Acros, and was purified by passing the liquid through a short column of basic alumina. Tetrahydrofuran (OmniSolv) and acetonitrile (Fisher) were dried over type 3A molecular sieves. Sulfuric acid (Fisher), ferric chloride (Fisher), perchloric acid (Sigma-Aldrich), anhydrous magnesium sulfate (Fisher), glacial acetic acid (Fisher), copper(II) chloride (Alfa Aesar), silver nitrate (Fisher), lithium perchlorate (Sigma-Aldrich) were all used as received. Pellethane 2103-70A (Dow Chemical) pellets (not dried) were dissolved in THF to

make a stock solution at a concentration of 87 g in 700 mL.

YLI Wash-A-Way basting thread was used as the water-soluble poly(vinyl alcohol) string.

2.3 Coated Poly(vinyl alcohol) Threads

2.3.1 Background

Poly(vinyl alcohol) (PVA) is a thermoplastic that is soluble in water but insoluble in most organic solvents. As such, PVA threads can be coated with the THF-based metastable polypyrrole solution. After the polymerization reaction has completed, dissolution of the PVA thread in water should leave a hollow PPy tube. All organic, electrically conductive hollow tubes are interesting for a number of potential applications (such as sensors and electrochromic patches), but more importantly these tubes serve as a proof-of-concept for more complicated structures formed through this templating approach.

2.3.2 Coating methods

2.3.2.1 preparation method one

A solution of approximately 1.1 g (0.50 mmol) PMA in 10 mL of THF was combined with a solution of around 70 mg (1 mmol) of purified pyrrole, yielding the metastable reaction solution. A number of PVA threads having approximately the same length were dipped in the solution for around five seconds, and then were clipped to a wire “clothesline” to dry. Some threads were rinsed with methanol after drying, some were not. Thicker coatings were formed by repeating the process a number of times.

2.3.2.2 preparation method two

A metastable reaction mixture was prepared by combining a solution of approximately 2.2 g (1 mmol) of PMA in 20 mL of THF with a solution of around 0.14 g (2 mmol) of pyrrole in 20 mL of THF. A length of PVA thread was held between two pairs of tweezers, and dipped into the reaction mixture. After drying, the thread was dipped again several times to build up PPy thickness.

2.3.2.3 preparation method three

The initial stages are similar to method two, except several PVA threads were treated simultaneously by wrapping both ends around pipette tips and dipping the whole assembly at once. Coating was built-up by repeated dipping, as many as thirty times.

The threads were post-processed with a variety of solutions in an attempt to change their conductive properties. Three oxidant solutions were prepared to modify the density of charge carriers along the polymer backbone. These solutions consisted of approximately

2.56 g (0.015 mol) of $\text{CuCl}_2 \cdot 2\text{H}_2\text{O}$ dissolved in 30 mL of H_2O , MeOH, or THF. A fourth solution containing 0.5 g (0.005 mol) lithium perchlorate in 30 mL of THF was prepared, the purpose of which was to infuse the polymer coating with an abundance of ions.

The dried, coated threads were cut into equal size pieces, and each was dipped into at least one of the four solutions for approximately five seconds and then hung to dry.

2.3.3 Results

2.3.3.1 method one

Several threads were prepared using method one (Section 2.3.2.1) with one to five PPy layers. All exhibited extremely high resistance. Scanning electron microscope (SEM) images are shown in Figure 10. It is worth noting that the specimens were sufficiently conductive to dissipate the beam charge from the scanning electron microscope, and none was gold coated.

Comparing Figures 10(a) and 10(b), there appears to be a denser coating on strings when there was no methanol rinse between coats. While the coated thread appears to be quite robust, removal of the PVA core leads to collapse of the PPy coating, illustrated in Figures 10(c) and 10(d). The structure in Figure 10(c) had not been rinsed with methanol between coatings, and the resulting thicker layer is reflected in the partial retention of structure after dissolution of the underlying thread; ruptured tubes are clearly visible. In the case where the thread was rinsed with methanol between coatings, complete disintegration of the tubes followed removal of the PVA thread, shown in Figure 10(d).

2.3.3.2 methods two and three

Threads coating by methods two and three (Sections 2.3.2.2 and 2.3.2.3) are presented in Figures 11(a) and 11(b), respectively. Neither was rinsed with methanol between layers. The thread in Figure 11(a) had the poly vinyl alcohol thread dissolved while the thread in Figure 11 did not. In the former case, it is clear that the build-up of PPy gave a coating that was sufficiently thick and robust to allow removal of the PVA core. However, the structures were still very fragile and any handling caused them to fall apart; the structure in Figure 11(a) was formed by soaking the coated fibres in water *after* they had been adhered to the SEM stub.

Table 2 summarizes the effects of treating 30-layer threads. Inconsistencies in coating thickness and test lead position led to significant experimental error, so the resistance measurements should be considered qualitative only.

Post-treatment appears to improve conductivity, whether it be with the mildly oxidizing CuCl_2 (#2,3,4,8,9,10) or with LiClO_4 (#5,6,7). It is not clear at this point whether this improvement in charge mobility is due to the reagents or simply the rinsing that accompanied

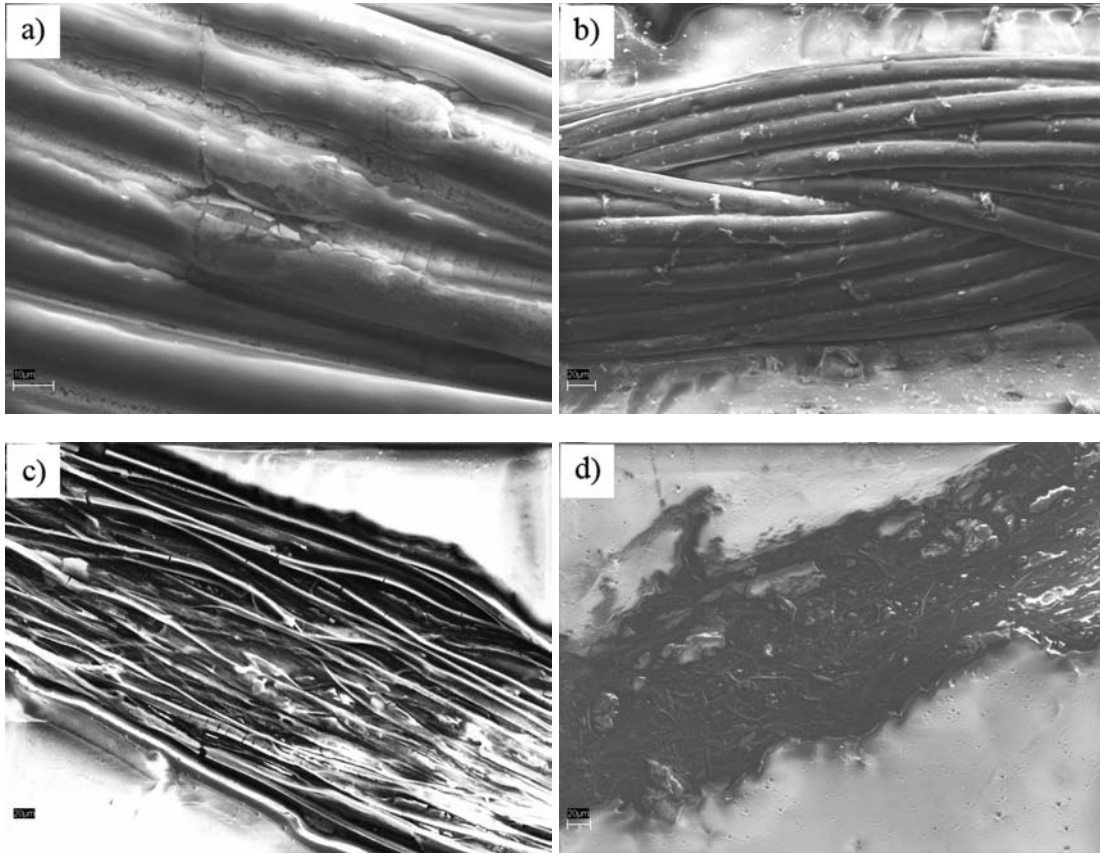


Figure 10: SEM images of PVA threads coated with five layers of polypyrrole, using the method as described in Section 2.3.2.1: (a) 1300 \times , thread not rinsed with MeOH between layers, PVA thread not dissolved; (b) 1140 \times , thread rinsed with MeOH between layers, PVA thread not dissolved; (c) 1100 \times , thread not rinsed with MeOH between layers, PVA thread dissolved; (d) 1200 \times , thread rinsed with MeOH between layers, PVA thread dissolved.

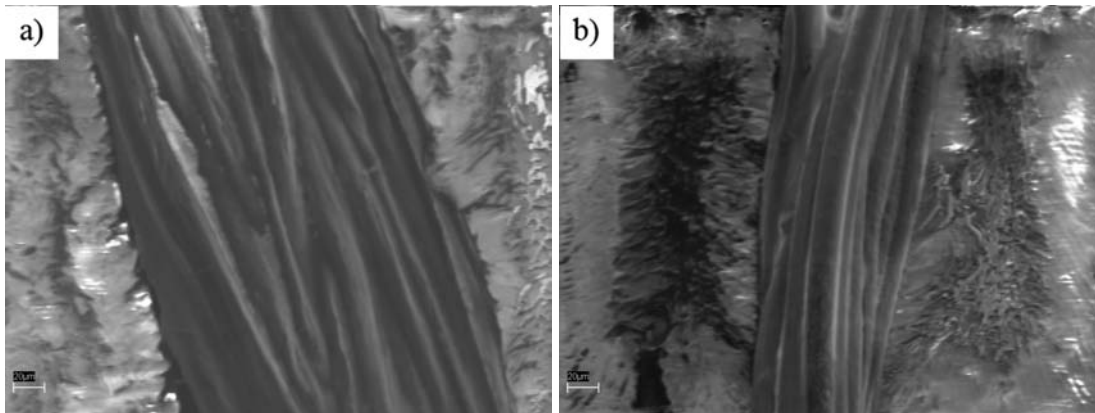


Figure 11: PVA threads coated in 30 layers of polypyrrole, and neither rinsed with methanol between layers: (a) 1000 \times , PVA thread dissolved; (b) 1000 \times , PVA thread not dissolved.

Table 2: Resistance (over 1 cm) of various polypyrrole-coated poly vinyl alcohol threads as measured with a multimeter. Each thread was coated with 30 layers of polypyrrole. None of the threads was rinsed with MeOH between coats.

#	Initial R (M Ω)	Treatment 1	R (M Ω)	Treatment 2	R (M Ω)
1	12	—	—	—	—
2	13	CuCl ₂ in H ₂ O	6	—	—
3	16	CuCl ₂ in MeOH	1.6	—	—
4	6.2	CuCl ₂ in THF	3.2	—	—
5	16	LiClO ₄ in THF	4	CuCl ₂ in H ₂ O	10
6	7	LiClO ₄ in THF	4	CuCl ₂ in MeOH	0.6
7	9.5	LiClO ₄ in THF	7	CuCl ₂ in THF	5.2
8	3	CuCl ₂ in H ₂ O	1.6	LiClO ₄ in THF	19
9	1.2	CuCl ₂ in MeOH	0.9	LiClO ₄ in THF	0.7
10	6.3	CuCl ₂ in THF	7.3	LiClO ₄ in THF	4.7
11	4.4	LiClO ₄ in THF	2.6	—	—
12	12	CuCl ₂ in H ₂ O	—	CuCl ₂ in H ₂ O	52
13	13	CuCl ₂ in MeOH	—	CuCl ₂ in MeOH	4
14	5	CuCl ₂ in THF	—	CuCl ₂ in THF	8

treatment. LiClO_4 appeared to have only a slight benefit when it was used in a second treatment (#9,10), but in one case it caused serious deterioration (#8). Similarly for CuCl_2 , the second treatment could improve conductivity (#6,13), decrease it (#5,12), or have no appreciable effect (#7,14). It is encouraging to note that post-processing experiments involving water (#5,12) likely resulted in dissolution of the PVA core, leading to structures such as those shown in Figure 11, although with somewhat worse resistance.

It is quite clear that the resistances are very high, despite the seemingly good coverage of the PPy layer. This could be due to the thinness coating. It could also be due to the brittle nature of polypyrrole, since any sort of mechanical disturbance to the structure (*e.g.*, moving the thread) will likely cause cracks in the polymer and disturb the conductive pathway. Samples where the supporting core had been dissolved would be particularly vulnerable. This problem might be overcome by using a polypyrrole/polyurethane composite which would have superior mechanical properties.

2.4 Glass Slides

2.4.1 Background

To illustrate the broad applicability of cascade polymerization, Polypyrrole was deposited on glass slides. The films were treated with a number of different substances in an attempt to decrease their resistance, as measured with a multimeter or a four-point probe.

2.4.2 Methods

Generally, the metastable reaction mixture was prepared from two solutions. One contained approximately 1.1 g (0.5 mmol) of PMA in 10 mL of THF. The other contained around 70 mg (1 mmol) in 10 mL of THF. Any additional components were added either to one solution before mixing, or to the combined reaction mixture, as detailed below. The final mixture was dropped onto a glass microscope slide and allowed to dry and react.

1. No additional treatment
2. AgNO_3 : 0.0220 g (0.13 mmol) of AgNO_3 was added to the PMA solution.
3. Glacial acetic acid (1): Approximately 1 mL of glacial acetic acid was added to the combined mixture.
4. Glacial acetic acid (2): One drop of glacial acetic acid was added to the combined mixture.
5. HClO_4 : 1 drop of perchloric acid was added to the combined mixture.
6. CuCl_2 and HClO_4 : 0.0223 g (0.13 mmol) of $\text{CuCl}_2 \cdot 2\text{H}_2\text{O}$ was added to the PMA solution. The solutions were mixed and 1 drop of perchloric acid was added.

7. CuCl₂ (1): 0.17 g (1.0 mmol) of CuCl₂ · 2 H₂O in 10 mL H₂O was added to the PMA solution.
8. CuCl₂ (2): 0.0219 g (0.13 mmol) of CuCl₂ · 2 H₂O was added to the PMA solution.
9. FeCl₃ and CuCl₂: 0.0204 g (0.13 mmol) of CuCl₂ · 2 H₂O was dissolved into the PMA solution and 0.0214 g (0.13 mmol) FeCl₃ in 5 mL of THF was added.
10. FeCl₃ (1): 0.0212 g (0.13 mmol) of FeCl₃ was dissolved into the combined mixture.
11. FeCl₃ (2): Anhydrous MgSO₄ was used to dry all the THF. 0.0221 g (0.13 mmol) of FeCl₃ was added to the combined mixture.
12. FeCl₃ (3): 0.0228 g (0.14 mmol) of FeCl₃ in 5 mL THF was added to the combined mixture.
13. MgSO₄ was added to each solution and filtered. The filtrates were mixed to create the metastable solution.

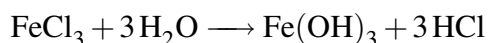
2.4.3 Results

Resistance data is summarized in Table 3. Semi-quantitative resistances were measured with a multimeter over a distance of around 1 cm. More rigorous surface conductivity was measured using a four-point probe device. Table entries denoted by a dash indicate resistance outside the range of the measuring apparatus.

Some post-treatments had either no effect or only a slight (and possibly insignificant¹) decrease in resistance (#2,5,8) compared to the blank (#1), while others led to a significant deterioration of the film's conductivity (#3,4,6,7). Only those treated with FeCl₃ (#9,10,11,12) showed any significant improvement.

The FeCl₃ results were initially somewhat surprising, since it was assumed that the addition of this strong oxidant would upset the initial conditions of the cascade polymerization, producing dimers earlier in the process, which in turn would drive the polymerization before the solvent had evaporated. This would presumably lead to poor quality polymers.

A possible explanation lay in the reaction of FeCl₃ with H₂O in the solvent, some of which originated from the water of hydration coming from the PMA crystals. This reaction consumes water, producing acid:



¹Since the measuring technique was not rigorous, any changes of less than ~ 50% were arbitrarily considered not significant.

Table 3: Multimeter (MM) and four-point probe resistance of treated polypyrrole films on glass slides, before and after rinsing with methanol.

#	Treatment	pre-rinse	post-rinse	
		R (k Ω) (MM)	R (k Ω) (MM)	R (k Ω / \square) (4-point)
1	none	260	16	20
2	AgNO ₃	290	15	11
3	Glacial Acetic Acid 1	2000	330	—
4	Glacial Acetic Acid 2	2900	2000	1000
5	Perchloric Acid	120	16	21
6	CuCl ₂ + HClO ₄	1500	—	—
7	CuCl ₂ + H ₂ O	2750	9000	—
8	CuCl ₂	135	8	20
9	CuCl ₂ + FeCl ₃	25	8	4
10	FeCl ₃	30	4	5
11	FeCl ₃	43	3	7
12	FeCl ₃	130	—	13
13	MgSO ₄	60	5	6

Since it was shown previously that pH has a strong influence on the redox potential of PMA [14], it was initially suspected that the acid was changing the polymerization kinetics. However, it was shown that added acid either leads to no significant contribution (#5) or damages the film severely (#3,4,6).

Alternatively, since FeCl₃ acts to dry the solvent, the removal of water could be the cause of improved polymer films. This is not surprising, since an abundance of water in the THF could interfere with the polymerization for a number of reasons. These include:

1. The polymerization process relies on the coupling of radical cations. In the current slow polymerization process, these radical cations are quite long-lived and in low abundance. If water, a nucleophile, is present, it will compete kinetically for the reactive monomers and oligomers, leading to shorter polymer chains and hence diminished conductivity. If this is the case, the rate law is likely first order in concentration of H₂O, suggesting that the effect will increase when more water is present. Nucleophilic attack of oxidized polythiophene by trace water is known [17], leading to substitution at the 3-position of the ring, disruption of conjugation, and subsequent loss of conductivity. Presumably, pyrrole is similarly vulnerable.
2. Polypyrrole is not soluble in water. The presence of water in the reaction mixture may cause the oligomers to precipitate prematurely. This would lead to shorter polypyrrole chains and hence lower conductivity.

3. The redox potential of PMA is sensitive to the nature of the solvent, including pH [14, 18]. The presence of water in the solvent will change the environment experienced by PMA (*e.g.*, dielectric constant) and so the redox potential will change. Furthermore, the presence of water will influence the dissociation constant of any acid present, again having an impact on the formal potential of PMA.

The wet solvent hypothesis is further supported by the observed increase in resistance in polymers formed in a solution deliberately spiked with water (#7) and a decrease in resistance when the metastable reaction was treated with a conventional drying agent, MgSO_4 (#13). Furthermore, it was noted that added water produced films that were brittle and crumbly, suggesting that the polymer chains were short and/or poorly formed.

2.4.4 Conclusions

Preliminary results indicate that better quality films can be deposited when the metastable reaction mixture is dried, either by a conventional agent such as MgSO_4 or by a reactive one such as FeCl_3 .

2.5 Polyurethane Composites

2.5.1 Background

Owing to factors such as a rigid backbone and extensive π -stacking, polypyrrole is a fairly brittle polymer. Previous work in this laboratory [14, 19, 20] has shown that Pellethane 2103-70A, a commercial thermoplastic polyurethane, is a robust matrix for forming conductive composites.

2.5.2 Method

Approximately 1.1 g (0.5 mmol) of PMA was dissolved in 10 mL THF using a 50 mL beaker. A second 50 mL beaker was used to dissolve approximately 70 mg (1 mmol) purified pyrrole in 10 mL THF. A third 50 mL beaker was used to prepare a Pellethane solution; this solution was added to the pyrrole solution and thoroughly mixed. Approximately 0.02 g (0.13 mmol) of FeCl_3 was added to the PMA solution. The Pellethane+Pyrrole and PMA+ FeCl_3 solutions were then mixed, spread onto a glass plate, and allowed to dry.

2.5.3 Results

None of the composite films was sufficiently robust to withstand extended handling. Lower weight fractions of pyrrole lead to more sturdy films at the cost of diminished conductivity, although none of the composites exhibited particularly good conductivity. Films cast on glass slides have resistance in the 2–4 $\text{M}\Omega$ range for composites having 25–66% w/w pyrrole.

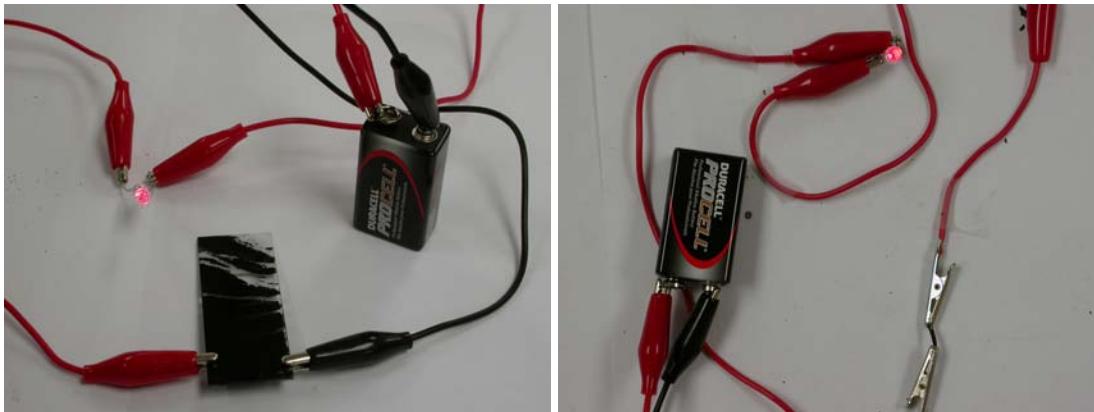


Figure 12: Examples of non-metallic wiring. Left: An FeCl_3 -doped polypyrrole film coated on a glass slide. Right: a length of freestanding polypyrrole composite “wire”.

2.5.4 Example applications of polypyrrole composites

All-organic polypyrrole composite conductors were assembled to illustrate a proof-of-concept. Figure 12 demonstrates two such examples: one film on glass and another as a free standing wire. While there is room for improving conductivity, these examples illustrate how the cascade polymerization method can be employed to create nonmetallic wiring.

2.6 Porous Polypyrrole

2.6.1 Background

In the past, Na_2SO_4 has been used as a porogen to create a porous polypyrrole film having superior electrochemical properties [15, 16]. The salt is insoluble in the reaction mixture but may be later dissolved from the film with water to leave behind a network of pores and channels through which electrolyte could flow. Because of this, there is greater counterion mobility within the conducting polymer. The corresponding decrease in ionic resistance allows for greater electrical currents to be developed within the polymer, which in turn makes the resulting material more attractive for use in high power applications such as supercapacitors.

In this alternate approach, the inert thermoplastic host in a interpenetrating network can serve as the template [14, 21]. In this case, a polypyrrole/polyurethane composite is used, and THF washes out the polyurethane. Naturally, the loading level of the composite affects the physical properties of the final material [20]; with too few pores, there may be no significant benefit, and with too many pores, the amount of conducting material may diminish to the point where electronic conductivity becomes compromised.

In the present work, CuCl_2 [14] was used as the oxidant.

2.6.2 Method

2.6.2.1 experimental

A stock solution of around 10% w/w Pellethane in THF was prepared. Appropriate quantities of this solution were added to a solution of purified pyrrole in THF. The resulting mixture was then combined with a solution of PMA in THF containing an adequate quantity of the reagent to yield the desired 1:2 PMA:pyrrole stoichiometry.

The solutions were thoroughly mixed. A Pasteur pipette was used to deposit two drops of the solution onto a glassy carbon electrode (CH Instruments, 3 mm diameter). Once dry, the film was soaked and rinsed repeatedly with THF to remove the Pellethane.

2.6.2.2 electrochemistry

The cyclic voltammetry (CV) and electrochemical impedance spectroscopy (EIS) measurements were obtained using a Solartron 1287 Electrochemical Interface and a Solartron 1260 Impedance/Gain-Phase Analyzer. Impedance spectra were acquired over a range of 0.1 Hz to 100 kHz with a 5 mV amplitude. CV and EIS experiments were performed in three-electrode configuration. The working electrode (porous polypyrrole coated glassy carbon) was submerged in an electrolyte solution of 0.1 M LiClO₄ in acetonitrile. A platinum wire was used as the counter electrode, and a KCl saturated calomel electrode was the reference. The entire system was deoxygenated with argon, and the experiments were run under an argon atmosphere.

2.6.3 Cyclic voltammetry

The cyclic voltammetry of a capacitor yields a rectangular $i - V$ curve in accordance with:

$$C = \frac{Q}{V} \quad (7)$$

$$= \frac{dQ/dt}{dV/dt} \quad (8)$$

$$= \frac{i}{v} \quad (9)$$

With capacitance corresponding to charge in the polymer film, and the introduction of ionic and electronic resistances, the CV of a conducting polymer resembles the rounded rectangle shape that a swept potential creates in an ideal RC circuit [22], shown in Figure 13a. A typical CV is presented in Figure 13b. The current at a given (slow) scan rate should be proportional to the quantity of electroactive material on the electrode (Equation 8).

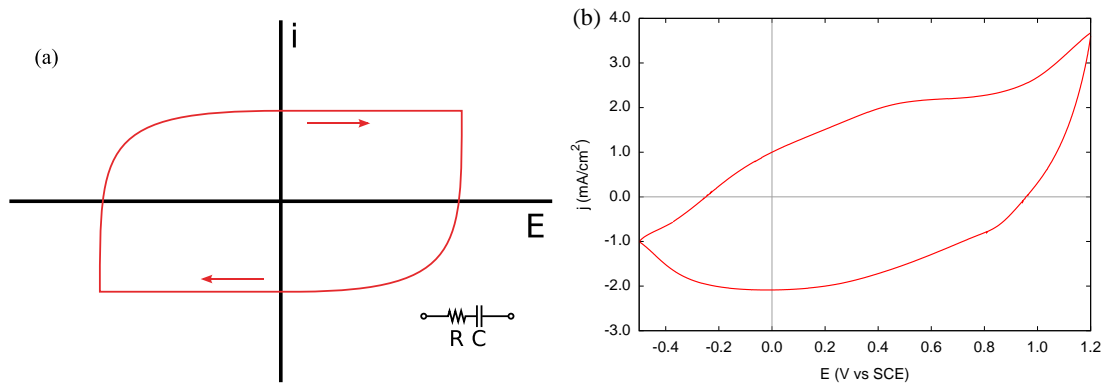


Figure 13: (a) Ideal voltammetric response of an RC circuit. When $R = 0$, the trace becomes rectangular, in accordance with Equation 9. (b) Representative cyclic voltammogram of polypyrrole on a glassy carbon disc electrode in MeCN/LiClO₄, $v = 10$ mV/s.

Table 4: Capacitance and ionic resistance of polypyrrole films of varying composition.

Loading %	i^* (mA)	C (mF)	Normalized C (C/mA)	R_i (Ω)
100	0.53	16	0.30	35
100	0.40	14	0.35	23
75	0.18	8.5	0.18	83
60	0.65	35	0.54	79
50	0.21	13	0.62	180

* From CV at 0.5 V, $v = 10$ mV/s

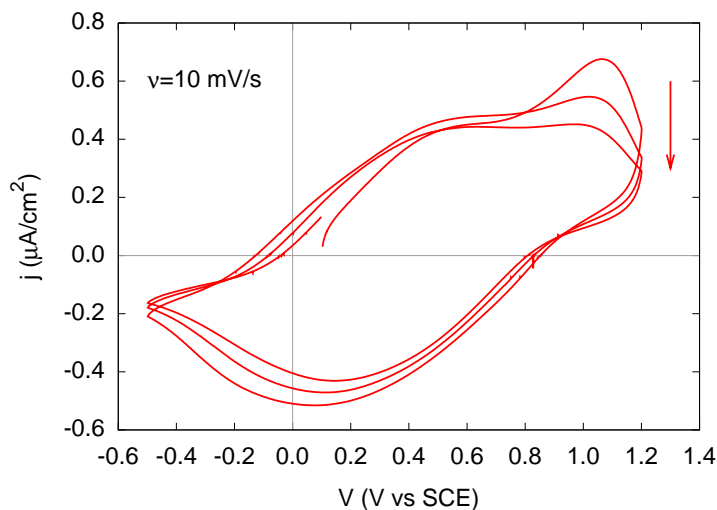


Figure 14: Representative degradation of a PPy film upon cycling at elevated potentials.

2.6.4 Impedance spectroscopy

A general introduction to impedance methods was presented earlier, in Section 1.2.2.

Table 4 summarizes R_i and C data for films of varying composition after having had the inert Pellethane guest dissolved. It is unclear whether a trend exists in the capacitance data. The “normalized” specific capacitance is not necessarily a good measure of true specific capacitance C_{sp} which would be normalized to the mass of active material. Since this was not known, the current from cyclic voltammetry was used as an estimate. However, since the current arising from a swept voltage is itself related to capacitance, using this property to normalize data may not be meaningful, and could explain why the values in Table 4 are quite close. Lastly, the impedance data were obtained after cycling to high potentials (1.2 V vs. SCE, see Figure 14) which presumably damaged the film to some extent.

The apparent ionic resistance follows a trend opposite to what might be expected; it appears to increase in the more open structures. It was also noted to be variable with potential, going through a minimum in the vicinity of 0.5 V, an example of which is shown in Figure 15. This second point is partly consistent with previous observations [23]; the oxidized sites along the polymer backbone leads to the incorporation of mobile anions and hence increased ionic conductivity. However, this does not account for behaviour at more elevated potentials. Electronic resistance could account for the resistance increase at higher potentials and in more diffuse films. If this is the case, then the simplified transmission line model (see Figure 3a) may not be valid here. Alternatively, if some Pellethane remained trapped within the matrix, it could fill some of the channels and act as a barrier between the polypyrrole and the electrolyte.

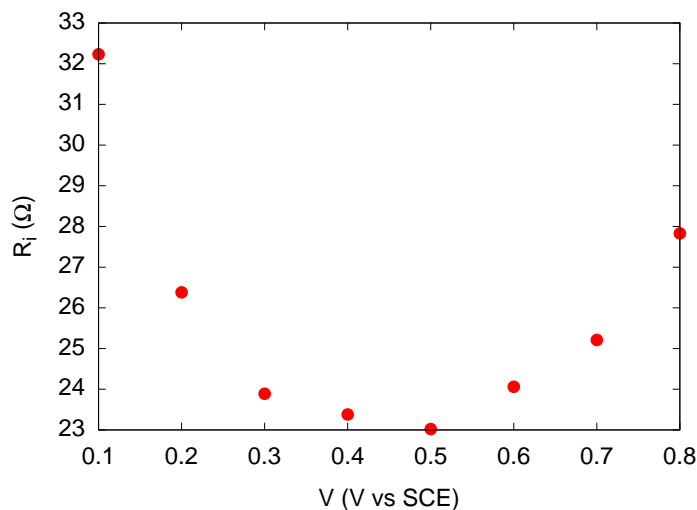


Figure 15: Variation in R_i with potential.

2.7 Polypyrrole Summary

Polypyrrole can be easily deposited on a water-soluble thread. Multiple dip-dry cycles allows for the build-up of layers to the point where the coating is sufficiently robust to leave hollow tubes when the core is dissolved. Poor conductivity was found, and this might be in part due to cracks forming in the brittle polypyrrole upon handling.

Films of polypyrrole cast on glass slides allow for straightforward comparison of the effects of different reaction conditions. It appears that the presence of water in the metastable solution leads to polymers of lower quality, and simply drying the component solutions with MgSO_4 produces satisfactory results.

Composites of polypyrrole and polyurethane have mechanical properties superior to polypyrrole alone. While conductivities are still not optimal, such composites were demonstrated as free-standing all-organic wires. It is not conclusive whether composite IPNs are useful as starting templates for porous polypyrrole.

Symbols and Abbreviations

- Square area of surface
- ϵ Dielectric constant
- v Sweep rate
- ω Frequency
- C Capacitance
- E Energy
- P Power
- Q Charge
- V Potential
- i Current
- t Time
- R_e Electronic resistance
- R_{high} Extrapolated high frequency resistance
- R_i Ionic resistance
- R_{low} Extrapolated low frequency resistance
- Z Impedance
- Z' Real component of impedance
- Z'' Imaginary component of impedance
- CFP** Carbon fibre paper
- CV** Cyclic voltammetry or voltammogram
- EIS** Electrochemical impedance spectroscopy
- ESR** Equivalent series resistance
- IPN** Interpenetrating polymer network
- MeCN** Acetonitrile

MeOH Methanol

PMA Phosphomolybdic acid

PPy Polypyrrole

PTFE Poly(tetrafluoroethylene); Teflon

PVA Poly(vinyl alcohol)

SCE Saturated calomel reference electrode

THF Tetrahydrofuran

TIF Technology Investment Fund

References

- [1] Andrukaitis, E., Bock, D., Eng, S., Gardner, C., and Hill, I. (2001), Technology Trends, Threats, Requirements, and Opportunities Study on Advanced Power Sources for the Canadian Forces in 2020, (Technical Report TR-2001-002) Defence R&D Canada.
- [2] Bull, R. A., Fan, F.-R. F., and Bard, A. J. J. (1982), *J. Electrochem. Soc.*, 129, 1009.
- [3] Pickup, P. G. (1990), *J. Chem. Soc. Faraday Trans.*, 86, 3631.
- [4] Ren, X. and Pickup, P. G. (1994), *J. Electroanal. Chem.*, 365, 289.
- [5] Cameron, Colin G. (2000), Enhanced Rates of Electron Transport in Conjugated-Redox Polymer Hybrids, Ph.D. thesis, Memorial University of Newfoundland.
- [6] Pickup, Peter G., Kalinathan, Karunakaran, Liu, Xiaorong, and DesRoches, Derrick (2008), Synthesis and Characterization of Modified Silicas and Carbons for Use as Electrodes in Electrochemical Supercapacitors: Second Annual Report, (CR 2008-090) Defence R&D Canada – Atlantic.
- [7] Conway, Brian E. (1999), *Electrochemical Supercapacitors*, Kluwer Academic.
- [8] Freund, M.S., Karp, C., and Lewis, N.S. (1995), Growth of thin processable films of poly(pyrrole) using phosphomolybdate clusters, *Inorg. Chim. Acta*, 240(1-2), 447–451.
- [9] Bravo-Grimaldo, Elda, Hachey, Sarah, and Freund, Colin. G. Cameron and Michael. S. (2007), Metastable reaction mixtures for the in situ polymerization of conducting polymers, *Macromolecules*, 40, 7166–7170.
- [10] Freund, Michael S. (2005), Controlled Chemical Polymerization Method for Processing Conducting Polymers: First Year Progress Report, (CR 2005-080) Defence R&D Canada – Atlantic.
- [11] Freund, Michael S. (2005), Controlled Chemical Polymerization Method for Processing Conducting Polymers Part 2: Final Report, (CR 2005-130) Defence R&D Canada – Atlantic.
- [12] Cameron, Colin G. and Freund, Michael S. (2005), Controlled Chemical Polymerization of Conducting Polymers, In *Proceedings of 11th CF/DRDC Meeting on Naval Applications of Materials Technology*, pp. 81–95. DRDC Atlantic SL 2005-192.

- [13] Cameron, Colin G., O'Hagan, Peter J., Suppes, Graeme, Deore, Bhavana, and Freund, Michael S. (2007), Conducting Polymer Composites and Their Derivatives, In *Proceedings of the 2007 CF/DRDC International Defence Applications of Materials Meeting*, pp. 41–47.
- [14] Cameron, Colin G. and O'Hagan, Peter J. (2006), The Effects of Pyrrole:Oxidant Ratios on the Permittivity of Conducting Polymer Composites, (TM 2006-208) Defence R&D Canada – Atlantic.
- [15] Freund, Michael S. (2007), Electrochemical Supercapacitors: First Annual Report, (CR 2007-199) Defence R&D Canada – Atlantic.
- [16] Freund, Michael S., Suppes, Graeme, and Deore, Bhavana (2008), Electrochemical Supercapacitors: Second Annual Report, (CR 2008-125) Defence R&D Canada – Atlantic.
- [17] Tsai, E. W., Basak, S., Ruiz, J. P., Reynolds, J. R., and Rajeshwar, K. (1989), Electrochemistry of some beta-substituted polythiophenes - anodic-oxidation, electrochromism, and electrochemical deactivation, *J. Electrochemical Soc.*, 136, 3683–3689.
- [18] Maeda, K., Himeno, S., Osakai, T., Saito, A., and Hori, T. (1994), A voltammetric study of keggin-type heteropolymolybdate anions, *J. Electroanal. Chem.*, 364, 149–154.
- [19] Cameron, Colin G., Underhill, Royale S., Rawji, Marc, and Szabo, Jeff P. (2004), Conductive filler – elastomer composites for Maxwell stress actuator applications, In *Proc. SPIE Smart Structures and Materials 2004: Electroactive Polymer Actuators and Devices*, Vol. 5385, pp. 51–59. DRDC Atlantic SL 2004-035.
- [20] Cameron, Colin G. and Mossman, Brody K. (2006), Dielectric, Morphological, and Electrochromic Properties of Conducting Polymer Composites, (TM 2006-209) Defence R&D Canada – Atlantic.
- [21] Freund, Michael S. (2005), Controlled Chemical Polymerization Method for Processing Conducting Polymers Part 2: Final Report, (CR 2005-130) Defence R&D Canada – Atlantic.
- [22] Bard, Allen J. and Faulkner, Larry R. (2001), *Electrochemical Methods*, 2 ed, Wiley.
- [23] Ren, X.M. and Pickup, P.G. (1995), Impedance measurements of ionic-conductivity as a probe of structure in electrochemically deposited polypyrrole films, *J. Electroanal. Chem.*, 396, 359–364.

Distribution list

DRDC Atlantic TM 2008-219

Internal distribution

- 2 Colin Cameron; 1 CD, 1 paper
- 2 Shayla Fitzsimmons; 1 CD, 1 paper (C/O Colin Cameron)
- 1 Trisha Huber
- 1 Ed Andrukaitis
- 1 Jeff Szabo, GL/MC
- 1 Leon Cheng, H/DLA
- 5 DRDC Atlantic Library

Total internal copies: 13

External distribution

- 1 Prof. Michael Freund
Department of Chemistry, University of Manitoba
Winnipeg, MB R3T 2N2
- 1 DRDKIM

Total external copies: 2

Total copies: 15

This page intentionally left blank.

DOCUMENT CONTROL DATA

(Security classification of title, body of abstract and indexing annotation must be entered when document is classified)

1. ORIGINATOR (The name and address of the organization preparing the document. Organizations for whom the document was prepared, e.g. Centre sponsoring a contractor's report, or tasking agency, are entered in section 8.) Defence R&D Canada – Atlantic P.O. Box 1012, Dartmouth, Nova Scotia, Canada B2Y 3Z7		2. SECURITY CLASSIFICATION (Overall security classification of the document including special warning terms if applicable.) UNCLASSIFIED	
3. TITLE (The complete document title as indicated on the title page. Its classification should be indicated by the appropriate abbreviation (S, C or U) in parentheses after the title.) Supercapacitor Separators and Polypyrrole Composites			
4. AUTHORS (Last name, followed by initials – ranks, titles, etc. not to be used.) Cameron, C.G.; Fitzsimmons, S.M.			
5. DATE OF PUBLICATION (Month and year of publication of document.) December 2008	6a. NO. OF PAGES (Total containing information. Include Annexes, Appendices, etc.) 40	6b. NO. OF REFS (Total cited in document.) 23	
7. DESCRIPTIVE NOTES (The category of the document, e.g. technical report, technical note or memorandum. If appropriate, enter the type of report, e.g. interim, progress, summary, annual or final. Give the inclusive dates when a specific reporting period is covered.) Technical Memorandum			
8. SPONSORING ACTIVITY (The name of the department project office or laboratory sponsoring the research and development – include address.) Defence R&D Canada – Atlantic P.O. Box 1012, Dartmouth, Nova Scotia, Canada B2Y 3Z7			
9a. PROJECT NO. (The applicable research and development project number under which the document was written. Please specify whether project or grant.) 12sz07	9b. GRANT OR CONTRACT NO. (If appropriate, the applicable number under which the document was written.)		
10a. ORIGINATOR'S DOCUMENT NUMBER (The official document number by which the document is identified by the originating activity. This number must be unique to this document.) DRDC Atlantic TM 2008-219	10b. OTHER DOCUMENT NO(s). (Any other numbers which may be assigned this document either by the originator or by the sponsor.)		
11. DOCUMENT AVAILABILITY (Any limitations on further dissemination of the document, other than those imposed by security classification.) (X) Unlimited distribution () Defence departments and defence contractors; further distribution only as approved () Defence departments and Canadian defence contractors; further distribution only as approved () Government departments and agencies; further distribution only as approved () Defence departments; further distribution only as approved () Other (please specify):			
12. DOCUMENT ANNOUNCEMENT (Any limitation to the bibliographic announcement of this document. This will normally correspond to the Document Availability (11). However, where further distribution (beyond the audience specified in (11)) is possible, a wider announcement audience may be selected.)			

13. ABSTRACT (A brief and factual summary of the document. It may also appear elsewhere in the body of the document itself. It is highly desirable that the abstract of classified documents be unclassified. Each paragraph of the abstract shall begin with an indication of the security classification of the information in the paragraph (unless the document itself is unclassified) represented as (S), (C), (R), or (U). It is not necessary to include here abstracts in both official languages unless the text is bilingual.)

The current trend of military forces worldwide is an increasing dependence on electrical power, and the Canadian Forces is no exception. Current technology, such as chemical sensors, radios, and portable computers, as well as rapidly emerging weaponry such as electromagnetic guns and directed energy weapons, demand increasingly sophisticated provision of electrical energy. Supercapacitors, for example, are ideally suited to supply large pulses of energy, and it is within the DRDC Technology Investment Fund project on supercapacitor materials that the current research has been undertaken.

This document reports the work of a summer student who studied two fundamental aspects of novel energy provision. First, a comparison of the low temperature performance of two different types of supercapacitor separator represents this lab's initial investigation into this niche area. It was found that a fixed pore separator outperforms a proton exchange membrane at low temperatures. Second, work with nanostructured polypyrrole composites builds on our earlier work in this interesting material, one which has numerous potential applications, including energy storage. Several concept structures are reported, including an all-polymer wire.

14. KEYWORDS, DESCRIPTORS or IDENTIFIERS (Technically meaningful terms or short phrases that characterize a document and could be helpful in cataloguing the document. They should be selected so that no security classification is required. Identifiers, such as equipment model designation, trade name, military project code name, geographic location may also be included. If possible keywords should be selected from a published thesaurus. e.g. Thesaurus of Engineering and Scientific Terms (TEST) and that thesaurus identified. If it is not possible to select indexing terms which are Unclassified, the classification of each should be indicated as with the title.)

This page intentionally left blank.

Defence R&D Canada

Canada's leader in defence
and National Security
Science and Technology

R & D pour la défense Canada

Chef de file au Canada en matière
de science et de technologie pour
la défense et la sécurité nationale



www.drdc-rddc.gc.ca